Biosensors and Bioelectronics 145 (2019) 111698

Contents lists available at ScienceDirect

Biosensors and Bioelectronics

journal homepage: www.elsevier.com/locate/bios

Epitope imprinting of *Mycobacterium leprae* bacteria *via* molecularly imprinted nanoparticles using multiple monomers approach

Archana Kushwaha[a], Juhi Srivastava[a], Ambareesh Kumar Singh[a], Richa Anand[b], Richa Raghuwanshi[c], Tulika Rai[d], Meenakshi Singh[a,*]

[a] Department of Chemistry, MMV, Banaras Hindu University, Varanasi, 221005, India
[b] Department of Applied Science, Indian Institute of Information Technology, Allahabad, India
[c] Department of Botany, MMV, Banaras Hindu University, Varanasi, 221005, India
[d] Department of Dermatology and Venereology, Institute of Medical Sciences, Banaras Hindu University, Varanasi, 221005, India

ARTICLE INFO

Keywords:
Epitope imprinting
Molecular imprinting
Electropolymerization
Quartz crystal microbalance
Mycobacterium leprae
Diagnostic tool

ABSTRACT

Mycobacterium leprae causes endemic disease leprosy which becomes chronic if not treated timely. To expedite this 'timely diagnosis', and that also at an early stage, here an attempt is made to fabricate an epitope-imprinted sensor. A molecularly imprinted polymer nanoparticles modified electrochemical quartz crystal microbalance sensor was developed for sensing of M*ycobacterium leprae* bacteria through its epitope sequence. Multiple monomers, 3-sulphopropyl methacrylate potassium salt, benzyl methacrylate and 4-aminothiophenol were utilized to imprint this bacterial epitope. Imprinted nanoparticles were electropolymerized on gold coated quartz electrode. The sensor was able to show specific binding towards the blood samples of infected patients, even in the presence of 'matrix' and other plasma proteins such as albumin and globulin. Even other peptide sequences, similar to epitope sequences only with two amino acid mismatches were also unable to show any binding. Sensor withstood analytical tests *viz.* selectivity, specificity, matrix effect, detection limit (0.161 nM), quantification limit (and 0.536 nM), reproducibility (RSD 2.01%). Hence a diagnostic tool for bacterium causing leprosy is successfully fabricated in a facile manner which will broaden the clinical access and efficient population screening can be made feasible.

1. Introduction

Diagnosis of any disease at an earlier stage is always better but for a chronic infectious disease, it has admirable benefits. Although mass healthcare industry is doing remarkable work in their respective R & D sectors but still many diseases remain undiagnosed till they reach to an incurable and fatal stage. As highlighted in the newspaper The Hindu Delhi, 10 Feb 2019; 90,709 cases of leprosy are reported in 2017–18 (The Hindu). WHO, 2004 has set the goal of zero children with leprosy and deformities by 2020. India was declared leprosy free after 2005 as the prevalence rate was 0.84% but after 2011, it was realized that the disease is very much around. *Mycobacterium leprae* is an obligate intracellular pathogen causing leprosy in humans. Diagnosis of the disease has been a challenge due to its long incubation period of 2–10 years and absence of specific tests. Serological tests based on the detection of antibodies specific for the phenolic glycolipid-I (PGL-I) antigen, a unique molecule of the *M. leprae* cell wall, does not work well in paucibacillary leprosy infected individuals (Martins et al., 2012; Spencer et al., 2005). Modern multidrug therapy and new antibiotics of proven efficacy have made it possible to meet the WHO's targeted reduction in the cause of *M. leprae* infection to a single case per 10,000 occupants in nations where the disease is endemic. Another pathogen, *Mycobacterium lepromatosis*, has recently been found to cause endemic disease in Mexico and the Caribbean (Han et al., 2009; Eichelmann et al., 2013). These developments call for new therapeutic points of view on the best way to adapt to an issue that is still a long way from resolved. A reasonable degree of certainty is required before making the diagnosis of leprosy. The era of genomic analysis has facilitated identification of *M. leprae* specific genes for designing tools for diagnosis. In the present study, *M. leprae* specific peptide was selected from studies done for diagnosis of sub or preclinical forms of leprosy based on the pattern of IFN-γ release of individuals' exposed or non-exposed to *M. leprae* (Martins et al., 2012).

If a diagnostic tool is devised which could detect the bacteria as soon as it infects the patients, its treatment could be carried out at nascent stage only and they will no more act as carrier of the disease for

* Corresponding author.,
E-mail addresses: meenakshi@bhu.ac.in, meenakshibhu70@gmail.com (M. Singh).

https://doi.org/10.1016/j.bios.2019.111698
Received 6 July 2019; Received in revised form 3 September 2019; Accepted 10 September 2019
Available online 12 September 2019
0956-5663/

another 2–10 years. Recently molecular imprinting fraternity is successful, at least at laboratory scale to detect virus, bacteria and other infection (disease) causing species in blood samples of patients at very low concentrations also through epitope imprinting (Yang et al., 2014; Nishino et al., 2006; Gupta et al 2016, 2018). Epitope imprinting has emerged as a viable alternative for protein imprinting, instead of using whole protein molecule as a template for imprinting, here only the peptide sequence from epitope region is imprinted (Ansari and Masoum, 2019; Lopez-Puertollano et al., 2019; Tchinda et al., 2019; Iskierko et al., 2019). Epitopes are 9–16 mer peptide sequences generally located on surface of proteins, facilitating the accessibility of protein through them thus making it convenient to capture the whole protein through them. Looking at the misery and scale of chronic infectious disease of leprosy, here we have fabricated an epitope imprinted sensor for *M. leprae* bacteria through the epitope sequence LP-15, predicted by Martins et al. for the first time (Martins et al., 2012).

Here, an attempt is made to device an epitope imprinted polymer matrix nanoparticles electrodeposited on gold coated quartz crystal electrode of EQCM to yield a piezoelectrogravimmetric sensor for *Mycobacterium leprae*. In this work, multiple monomers; 3-sulphopropyl methacrylate potassium salt, benzyl methacrylate and 4-aminothiophenol were used for knitting the polymeric imprinting framework. Epitope sequence from *Mycobacterium leprae* predicted by Martins et al. helped to recognize and bind the bacterium on imprinted surfaces of sensing device (Martins et al., 2012).

To further increase the amount of viable binding sites in sensor matrix, the simplest method is to provide a higher surface area to the polymer film, through the assembly of nanoparticles in the sensing film (Du et al., 2010; Vittal and Gomathi, 2002; Crespilho et al., 2006; Kumar et al., 2007). Here, in this work, nanosized moleculary imprinted polymers were generated and electrodeposited on electrode of piezoelectric transducer yielding a piezoelectric diagnostic tool facilitating 'real time' monitoring of infections in 'real' samples of patients. It is a simple, cost-effective, high resolution mass sensing device which has been preferred for analytical application due to its sensitivity to nanogram level of mass change adsorbed onto the surface of EQCM resonator.

2. Materials and methods

2.1. Reagents and materials

All chemicals and solvents were of analytical reagent grade and used without further purification. 4-aminothiophenol (4-ATP) (98.5%), 3-sulfopropyl methacrylate potassium salt (98%) and benzylmethacrylate (96%) were purchased from Sigma Aldrich (Steinheim, Germany). Azoisobutyronitrile (AIBN) (98%) was procured from Ottokemie (Mumbai, India). Potassium chloride (98.5%), disodium hydrogen orthophosphate (anhydrous) (99%) and sodium dihydrogen orthophosphate (dehydrate) (99%) were obtained from Fisher Scientific (Waltham, MA, USA). HCl (95%), H_2SO_4 (90%) and H_2O_2 (95%) were purchased from Merck Specialities Pvt Ltd. Potassium ferricyanide ($K_3[Fe(CN)_6]$) was purchased from Fisher Scientific Pvt Ltd. Potassium hydroxide (95%) was purchased from RFCL limited, New Delhi, India. The computationally derived epitope of *mycobacterium leprae* LDIYTTLARDMAAIP (Leu-Asp-Ile-Tyr-Thr-Thr-Leu-Ala-Arg-Asp-Met-ala-Ala-Iso-Pro) (LP-15) and their interferrants LDIYTARDMAAIP (Leu-Asp-Ile-Tyr-Thr-Ala-Arg-Asp-Met-ala-Ala-Iso-Pro) (LP-13), VQKAVGSILVAGC (val-gln-lys-ala-val-gly-ser-ile-leu-val-ala-gly-cys) (VC-13), KPYAKNSVALQAVC (lys-pro-tyr-ala-lys-asn-ser-val-ala-leu-glu-ala-val-cys) (KC-14), GRHNSESYHW (gly-arg-his-asp-ser-glu-ser-tyr-his-trp) (GW-10) and KPYAKNALQAVW (lys-pro-tyr-ala-lys-asn-ala-leu-gln-ala-val-trp) (KW-12) were synthesized and obtained from GL Biochem (Shanghai) Ltd, China. Human blood plasma samples were collected from Institute of Medical Science (IMS), Banaras Hindu University (BHU) (Varanasi, India) as per approved protocol by the institutional ethical committee of IMS, BHU after patients' written informed consent.

2.2. Instruments

All electrochemical measurements were performed on a CHI 410B electrochemical workstation with three electrode system (an EQCM gold electrode, a platinum wire and Ag/AgCl electrode were used as working, counter and reference electrodes respectively). EQCM containing a potentiostat/galvanostat (440B), an external box with oscillator circuitry and the EQCM cell was used. Two contact pins from the oscillator box is connected to the crystal holder of the EQCM cell. A gold electrode surface was coated on both faces of an 8 MHz AT-cut QCM chip. A seal is formed by two O-rings that are pressed by four screws. The diameter of the quartz crystal is 13.7 mm. The gold electrode coated on quartz crystal has a diameter of 5.11 mm. Electrochemical examination like cyclic voltammetry (CV) was performed on a CHI 410B electrochemical workstation with a traditional three electrode framework. A platinum wire (Pt) electrode and Ag/AgCl electrode have been used as counter electrode and reference electrode respectively.

Multi Autolab Cabinet M101 module, FRA32M Module, EQCM module for Multi Autolab Cabonet and EQCM MHz Pt/TiO_2 quartz crystal was employed for electrochemical impedance spectroscopy measurements. A magnetic stirrer (Ika model-C-MAG HS7), ultra sonicator (OSCAR Ultrasonic cleaner, Microclean-102) and cooling centrifuge (REMI model-C 24 BL) were employed to stir, sonicate and centrifuge the test solutions during measurements.

Static contact angles of water were measured using the sessile drop method by contact angle goniometer equipped with CCD camera (model HO-IAD-CAM-01) from Holmarc Opto Mechatronics Pvt Ltd. India.

Atomic force microscopy (AFM) images were taken using instrument Solver Next model of NT-MDT Company which is used for visualization and evaluation of surface dominant features. Contact mode with soft silicon nitride tip, covered with reflective gold coating on the back side, was used in order to obtain the topography images. The scanned area of the sample was 5 μm × 5 μm and scan rate of AFM was 0.5 Hz.

2.3. Experimental

2.3.1. Synthesis of epitope imprinted polymer nanoparticles

The synthesis of epitope imprinted and non-imprinted multifunctional polymer nanoparticles thin film included four steps (as shown in Scheme 1): (1) dissolving epitope sequence with multiple monomers bearing either one or two functional groups in suitable solvents, followed by addition of initiator (AIBN) for polymerization; (2) collection of nanoparticles of polymeric adduct *via* repeated ultrasonication and centrifugation; (3) with the aid of an electropolymerizable monomer (4-ATP), electropolymerization of polymeric adduct nanoparticles onto gold surface of EQCM electrode; followed by (4) extraction of template (epitope sequence) on exposure to PBS (25 mM of 7.3 pH) (Gupta et al., 2018). The non-imprinted polymer (NIP) thin films were prepared identically, except addition of epitope sequence in polymerization solution.

In detail, monomer 3-sulphopropyl methacrylate potassium salt (0.2 M; 0.24 g/5 mL acetonitrile), benzyl methacrylate (0.2 M; 0.178 g/5 mL acetonitrile), 4-ATP (0.2 M; 0.125 g/5 mL acetonitrile) were suspended with analyte (0.5 mM of epitope LP-15 (0.0034 g/5 mL in 20 mM PBS pH 7)), mixed well and left for self assembly with epitope sequence as analyte. This solution was stirred on water-bath at 65 °C and while stirring, AIBN was added as initiator drop-wise and stirring was continued for another 12 h. A polymeric adduct was formed, which was ultrasonicated for 2 h and then centrifuged (5000 rpm, 20 min). This cycle of stirring (30 min), ultrasonication (2 h) and centrifugation (5000 rpm, 20 min) was repeated for 8 times while maintaining their volume with acetonitrile to obtain nanoparticles of polymer adduct as verified by AFM images (~300 nm).

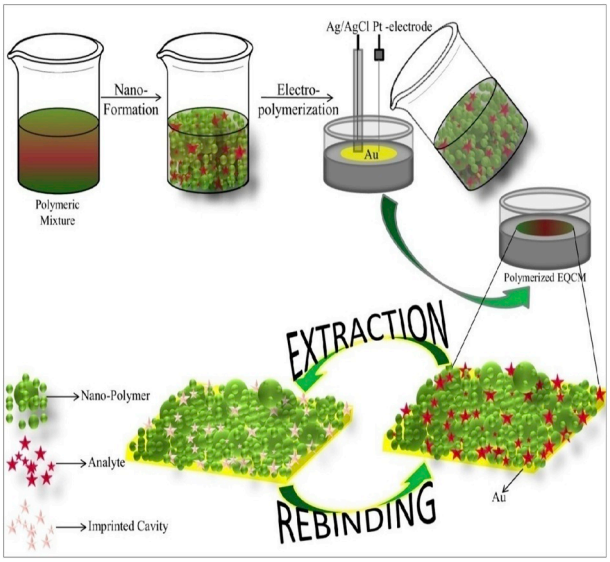

Scheme 1. Schematic representation for fabrication of analyte (LP-15) imprinted EQCM sensor.

2.3.2. Modification of EQCM electrode

EQCM electrode was immersed in piranha solution (H_2O_2/H_2SO_4 = 1/3) for 5 min, and rinsed with deionized water prior to use. Gold surface of EQCM electrode was exposed to the solution of polymer adduct nanoparticles prepared (discussed in above section) and CV cycles (12 cycles) were run in the range of +1.2 V to −0.6 V at scan rate 100 mV/s using KCl (0.1 mM) as supporting electrolyte to carry out electropolymerization of 4-ATP units present in polymeric adduct solution. Subsequently, EQCM electrode was rinsed with deionized water for removal of any physisorbed species.

2.3.3. Extraction of epitope sequence (LP-15)

The template (epitope sequence (LP-15)) was extracted by exposing the modified EQCM electrode with PBS (25 mM; pH 7.3) using EQCM run for 6 h by repetitive addition of PBS in EQCM cell to generate imprinted cavities on EQCM electrode (Gupta et al., 2018). This extraction was monitored by piezoelectric run (Fig. S1) as well as fluorescence spectra of extracted solution (Fig. S2).

2.3.4. Rebinding/adsorption of analyte at MIP and NIP modified EQCM electrodes

For the rebinding studies, a series of solutions with varying concentration of epitope was prepared and directly added to the electrochemical cell for analysis. For rebinding studies of analyte (LP-15) molecules towards MIP and NIP modified EQCM electrodes, a series of solution with different concentration of analyte was prepared in PBS (10 mM; 7 pH), varying from 10 to 140 nM and directly added to the electrochemical cell for analysis. The amount of epitope adsorbed was measured by change in resonating frequency as well as their mass deposition on EQCM electrode (Fig. S3). To demonstrate the reproducibility, results were averaged out of five consecutive measurements. Repeated adsorption (rebinding) and extraction were also monitored by decrease (Fig. S4) and increase (Fig. S1) in resonating frequency of modified EQCM electrode respectively.

For study of other experimental parameters crucial for rebinding like pH, etc., similar procedures were repeated by changing analyte solution pH (pH 6 to 8) using HCl and NaOH. LOD was calculated as three times the standard deviation from blank measurement (in the absence of epitope sequence) divided by slope of calibration plot between epitope sequence concentration and change in frequency (Skoog et al., 1998). Electrochemical measurements, as mentioned above, were also carried out with NIP EQCM electrodes under similar operating conditions. MIP and NIP modified electrodes were stored under refrigeration (~10^{O}C) when not in use.

2.3.5. Cross - selectivity study towards structural analogues, plasma proteins and infected patients' blood samples

To check the selectivity of epitope (LP-15) imprinted EQCM electrode, the influence of mismatched epitope sequences was examined under optimized experimental conditions. The mismatched sequences were comprised of amino acid residues present in imprinted sequences but with differing sequence, such as LP-13, GW-10, KC-14, VC-13, KW-12. Response of imprinted electrode towards other proteins present in blood plasma *viz.* globulin, albumin and concurrently *mycobacterium leprae* infected patients' blood samples were also tested. Solution of each of them (10 nM) was prepared in PBS (10 mM) and 0.3 mL was added in each step to EQCM cell. Infected blood serum of *mycobacterium leprae* bacteria as well as blood serum of healthy human being were analysed on thus fabricated EQCM sensor. The blood serum was stored in −20 °C and thawed in 4 °C before use. It was diluted sequentially with PBS buffer solution (10 mM, pH 7) before use.

2.3.6. Electrochemical impedance spectroscopy (EIS)

$K_3[Fe(CN)_6]$ (0.1 M) was employed as the electroactive probe, and PBS (0.1 M) was used as supporting electrolyte to investigate the sensing properties of the imprinted sensor with EIS followed by washing with deionized water. Afterwards, EIS estimation was carried out through a redox probe *i.e.* 1 mL of $K_3[Fe(CN)_6]$ solution was added on adduct, MIP film coated and NIP film coated EQCM electrodes and their impedance spectra were measured to check the conductivity of prepared sensor (Fig. S5).

2.3.7. Indirect estimation through electroactive probe

For rebinding studies at modified electrodes, 1 mL of $K_3[Fe(CN)_6]$ (0.1 M) solution was added on EQCM electrodes prior to DPV run in the presence of 0.25 mM PBS as supporting electrolyte, followed by analyte solution. The response of redox probe towards the MIP modified EQCM sensor was estimated by decrease in the current response of DPV run on each addition of analyte (Fig. S6). To analyse the characteristic features of modified films, 1 mL of $K_3[Fe(CN)_6]$ (0.1 M) solution was added on bare gold electrode, adduct, MIP film coated and NIP film coated EQCM electrodes each and their DPV currents were evaluated to check the conductivity of prepared sensor (Fig. S7).

3. Results and discussion

3.1. Synthesis of epitope imprinted polymer nanoparticles

Polymerization of monomers (except 4-aminothiophenol) with epitope (LP-15) were carried out in bulk as per protocol given in reference (Gupta et al., 2018), the only variation is addition of template in prepolymerization mixture. Monomers chosen for imprinting were 3-sulfo propyl methacrylate potassium salt, benzyl methacrylate and 4-aminothiophenol (as conducting and electroactive monomer). 3-Sulfo propyl methacrylate potassium salt and 4-ATP have sulphur atoms which facilitates grafting of polymeric matrix onto the gold surface of EQCM electrode through well known chemistry of thiols to self assemble on gold surface. Polymerization was carried out in presence of monomers and AIBN as initiator. Nanosized particles of formed polymeric adduct was collected by repeated stirring, ultrasonication and centrifugation of adduct (Fig. S8 showing nanosize, (Scheme 1)). Nanoparticles have high surface area facilitating a better accessibility to analyte molecules.

AFM images of modified EQCM electrodes are shown in Fig. S8 (c,d). Particles sizes are in the range between 200 and 300 nm and average size was 209–276 nm (Fig. S8, Table S1). MIP film displays rough surface with a number of cavities while smoother surface is observed on NIP modified electrode surface, although

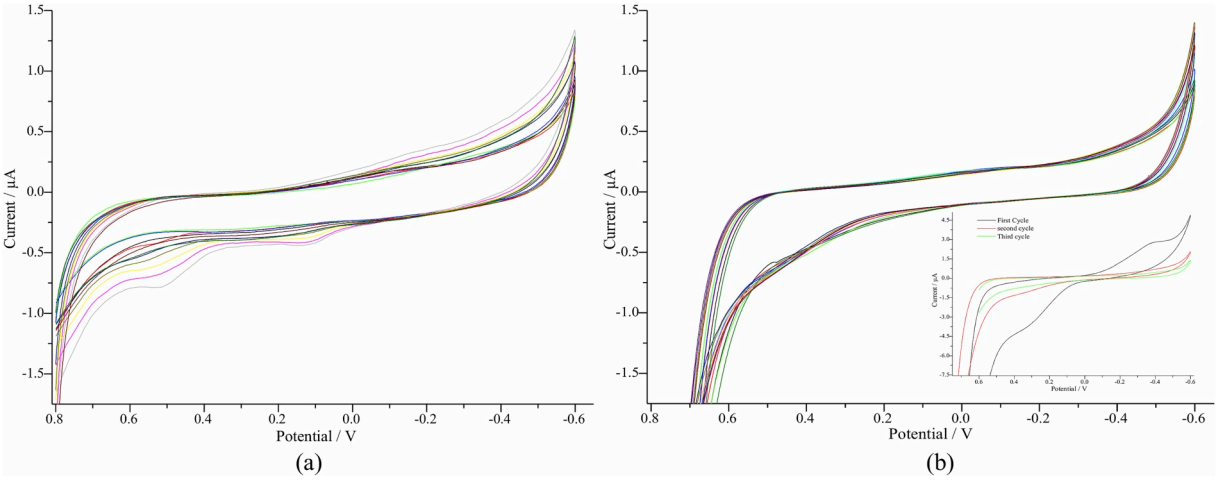

Fig. 1. CVs of electropoymerization of (a) epitope (LP-15) bound polymer (adduct), (b) non-imprinted polymer [inset graph represents the first, second and third cycles] solution on gold coated EQCM electrode from range 0.8 to −0.6 V at scan rate 0.1 V/s for 12 cycles in the presence of 0.1 mM of KCl as supporting electrolyte. (For interpretation of the references to colour in this figure legend, the reader is referred to the Web version of this article.)

electropolymerization of both MIP and NIP polymeric matrix were carried out under identical experimental conditions except in presence and absence of epitope sequence only. Thickness of MIP film deposited at gold surface is around 25–35 nm (z-axis; Fig. S9). The images of formed cavities on MIP film demonstrate their depth as nearly 10–15 nm (Fig. S10, Table S1).

3.2. Electropolymerization onto gold surface of EQCM electrode and its characterization

Cyclic voltammograms for electropolymerization of polymer nanoparticles is shown in Fig. 1. Polymer nanoparticles were electropolymerized at cathodic potential of 0.517 V, 0.145 V, 0.2622 V and anodic potential at −0.111 V showing appreciable enhancement in current with each scan as polymerized layer became thicker with concomitant scan (Raj et al., 2001; Lukkari et al., 1998). In the initial cycles, the current change was significantly recognizable and current reached to its saturated value in 12 cycles, demonstrating a stabilized layer deposition onto gold coated EQCM electrode. 4-ATP is used here as an electropolymerizable component helpful in electrodeposition of nanoparticles. Mass loading on electrode in each electropolymerization cycle of MIP and NIP was found to saturate in 12 cycles; hence number of cycles was kept to12 for further experimentation.

Extraction of epitope molecules from the polymeric film was followed by monitoring resonating frequency of quartz crystal of EQCM electrode (Fig. S1). On extraction of analyte from imprinted polymeric film, resonating frequency enhance as the template molecules are getting released from polymeric matrix on exposure to extractant solution and template specific cavities left behind contribute to selective capture of analyte molecules. To further monitor extraction of epitope sequences from polymeric matrix, fluorescence spectrum, another suitable technique was used (Fig. S2). In the *Mycobacterium leprae* protein's epitope sequence LDIYTTLARDMAAIP, tyrosine (Y) is present which fluoresces when excited with UV light; shows excitation with wavelength 274 nm. Fig. S2 presents the fluorescence spectra of fresh solution of epitope molecule (in PBS) and extracted solution from polymeric film. The absorption study of epitope sequence showed a characteristic absorption peak centered at 274 nm wavelength *i.e.* ranging from 272 to 550 nm (excitation wavelength 305 nm) with high intensity and sharp peak and extracted solution also shows absorption peak with a lower intensity and broader peak in the same range (Fig. S2) (Held, 2003). Thus the study of absorption/emission spectra of epitope and extracted solution clearly shows that epitope molecules were extracted from polymeric matrix leaving behind epitope imprinted cavities in polymeric matrix on gold surface of EQCM electrode.

Contact angle measurements were also used to verify the change in nature of surface on formation of imprinted sites on EQCM electrode. Table S2 shows the contact angles of water on adduct coated, MIP-coated, NIP-coated and bare gold EQCM electrode. Contact angles of water on bare gold EQCM electrode (73.63°) decreased on formation of adduct *i.e.* EQCM electrode electropolymerized with MIP and NIP nanoparticles, with and without analyte (30.17°) respectively, which predicts hydrophilicity. On extraction of analyte molecules, functional groups of monomers (now polymer) tethering the template molecule with their respective complementary functional groups are left behind bare, extending hydrophobicity to the electrode surface (49.82°) in comparison to adduct or NIP coated electrode surface. Hence, the hydrophobicity of MIP modified surface corroborates the creation of imprinted cavities on polymeric matrix (Fig. S11).

3.3. Rebinding of epitope sequences onto imprinted EQCM electrode

Fig S4 shows the piezoelectrogravimmetric response of modified EQCM electrode on sequential addition of epitope solution in concentration range 10–140 nM till saturation. Binding of epitope sequence was also illustrated by mass loading suggesting adsorption of analyte in specific cavities of MIP film coated EQCM electrode. Simultaneous recording of resistance change of modified electrode shows insignificant change, thus attesting the compact binding of analyte epitope sequences in imprinted cavities (Fig. S3). In case of non-specific bindings, analyte sequence easily drifts away on any weak stimulus culminating large changes in resistance of EQCM electrode showing high viscoelasticity. Hence, committed specificity of imprinted cavities for analyte sequence is validated.

3.4. Response of imprinted EQCM sensor towards pH

pH of analyte solutions is a critical parameter influencing the nature as well as conformational geometry of analyte sequence in addition to that of imprinted cavities. Thus, the influence of pH was examined in the range of 6–8. Rebinding is optimum at pH 7.5 and binding is weakened on either side *i.e.* on moving towards slightly acidic (pH 6) or slightly alkaline (Fig. S12). Under slightly alkaline condition, the amino groups of epitope and acrylic group of monomers are all in the molecular state and can easily form hydrogen bonds; subsequently, the highest adsorption efficiencies were achieved at pH 7.5. At lower pH values (pH 6.0) of analyte solution, since there is no functional group available to be protonated to form an ionic state resulting in lesser

binding. Consequently, pH 7.5 was chosen as analyte solution pH for subsequent experiments.

3.5. Indirect estimation of electrochemical responses of MIP, NIP and bare gold electrodes

A redox probe $K_3[Fe(CN)_6]$ was used to examine the nature of imprinted films as well as indirect estimation of analyte (Fig. S6 (a - l)). Fig. S7 depicts the conduction of this redox probe on NIP-film coated EQCM electrode (curve a), bare EQCM electrode (curve b), after extraction of epitope molecules *i.e.* MIP (curve c) and before extraction of analyte *i.e.* adduct (curve d). Response of NIP on gold electrode (curve a) corroborates conducting nature of NIP film *i.e. p*-ATP; their conducting nature enhances the conductivity of NIP coated film to facilitate electron-transfer towards the electrode surface (Raj et al., 2001; Lukkari et al., 1998). In curve (d), lower current of DPV response is obtained in comparison to NIP as epitope molecules are anchored in polymeric film, thus probe molecules are not able to reach the surface of electrode to show its electroactivity. In MIP film, on extraction of analyte sequences, imprinted cavities are generated which facilitates the movement of probe molecules through them and redox probe could display its electroactivity (curve c). The pathways of probe molecules to reach at electrode surface are hindered on rebinding of analyte molecule as these imprinted sites are again occupied by analyte sequences. Accordingly by probing electrochemical activity of the $[Fe(CN)_6]^{3-/4-}$ redox couple at the modified EQCM electrode, using DPV can indirectly determine the epitope level (Fig. S6).

3.6. Electrochemical impedance spectroscopy (EIS) of EQCM electrodes

EIS studies of modified EQCM electrode in presence of a redox probe $K_3[Fe(CN)_6]$ were investigated. The obtained results are shown in Fig. S5 as Nyquist plot. Nyquist plot, also known as Cole–Cole plot, comprises a semi-circle region lying on the axis followed by a straight line as the frequency approaches lower values. The semicircle portion in the higher frequency region corresponds to the charge-transfer process whereas the straight line part in the lower frequency region represents diffusion controlled process. Fig. S5 shows the impedance plot on EQCM electrodes coated with MIP film (before and after extraction of analyte), and NIP modified EQCM electrode. The impedance plot manifested that the resistance offered by MIP-modified electrode after extraction (curve 'a') is low. This high conductivity of electrode surface (owed to 4-ATP) permits electroactivity of redox probe. Curve 'b' demonstrates the plot for MIP-modified electrode before extraction (adduct) while curve 'c' shows the corresponding plot for NIP-modified electrode. NIP-modified electrode indicates complete coverage of electrode surface which does not facilitate any movement of probe molecules to EQCM electrode surface thus enhancing the impedance as shown in Fig. S5 (curve 'c'). While MIP-modified electrode obtained after extraction (curve 'a') shows lesser impedance than MIP-modified electrode before extraction (curve 'b') of analyte. Cavities created in imprinting matrix paves the path for redox probe molecules to contact electrode surface for electroactivity.

3.7. Binding affinity towards MIP and NIP modified EQCM electrodes

Fig. 2 represents EQCM response for rebinding of analyte molecules (LP-15) on MIP film modified electrode. The resonating frequency decreases continuously on successive addition of analyte solution in concentration range 10–140 nM. It is obvious from Fig. S4, decrement in resonating frequency on every addition of analyte indicates capture of analyte sequences on specific imprinted cavities and concurrent mass deposition on sensor electrode. The respective change in resistance of quartz crystal (EQCM electrode), visualizing viscoelasticity of coated film on quartz surface occurs to an insignificant extent, as analyte molecules are bound firmly using specific interactions through

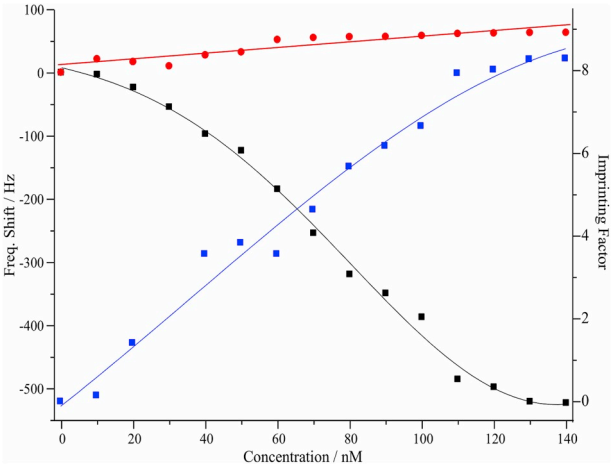

Fig. 2. Rebinding of analyte molecules on MIP-coated EQCM electrode (■), NIP-coated EQCM electrode (●) at various concentrations of epitope (LP-15) with their calculated imprinting factor (IF) (■).

complementarity of respective functional groups, those left behind in polymeric matrix after extraction and those present on analyte sequence (inset of Fig. S4). The extent of imprinting and specificity of prepared MIP sensor is also estimated by imprinting factor (IF):

$$I.F. = \frac{(\Delta f)_{MIP}}{(\Delta f)_{NIP}} \quad (1)$$

where Δf_{MIP} = frequency change on addition of analyte onto MIP modified EQCM eletrode and Δf_{NIP} = frequency change on addition of analyte onto NIP modified EQCM eletrode.

Change in resonating frequency is displayed in Fig. 2 for rebinding on MIP nanoparticles modified and NIP nanoparticles modified EQCM electrode with their imprinting factor at each concentration. Selective recognition towards the analyte (LP-15) molecule has prevailed in MIPs sensor. For this epitope imprinted polymer coated EQCM sensor, IF is calculated to be 8.28 at concentration 140 nM under optimized conditions which validates high specificity towards imprinted epitope sequence. Although functional groups of monomers responsible for imprinting were also present in non-imprinted matrix, however the guided orientational movement induced by complementary functional groups of analyte towards 3D spatial contours of imprinted polymeric network is lacking in non-imprinted network, thus unable to incite the analyte molecules' movement towards the functional groups present in non-imprinted matrix. In imprinted matrix, analyte molecules leave behind their 'imprint', *i.e.* the guided conformational orientation of functional groups piloting the analyte molecules towards specific imprinted cavities.

3.8. Adsorption isotherm

MIPs are usually characterized utilizing adsorption isotherm equations because a target-MIP interaction depends on the binding equilibrium of analyte molecule and analyte-selective cavities created in the polymeric matrix (Spivak, 2005). Hence, the adsorption isotherm equations for a heterogeneous distribution, such as, Freundlich adsorption isotherm (a power function, where 'a' and 'm' are constants) is often utilized (Eq. (5.1)) (Umpleby et al., 2004). Isotherms of this form have been observed for a wide range of heterogeneous surfaces. By using these equations, the binding affinity as well as the homogeneity of the binding-site distribution can be evaluated (Spivak, 2005).

Garcıa-Calzon and Dıaz-Garcıa stated, that continuous distribution model is the uniformly accepted Freundlich isotherm presented by HMF Freundlich as an empirical sorption isotherm for non-ideal sorption on heterogeneous surfaces and multilayer sorption (Garcıa-Calzon and

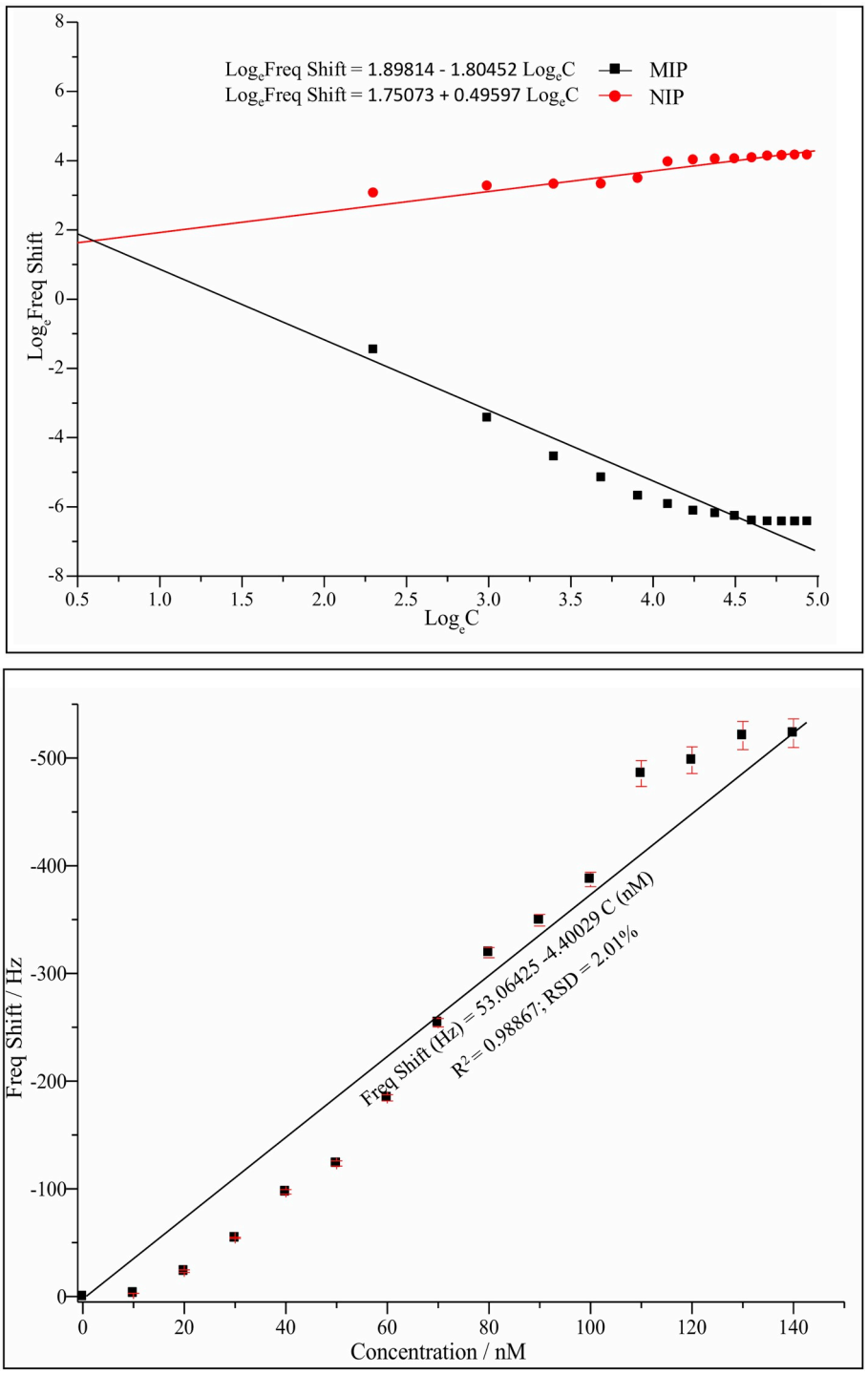

Fig. 3. (a) Binding adsorption isotherm for MIP [Log$_e$Freq Shift = 1.89814–1.80452 Log$_e$C] and NIP [Log$_e$Freq Shift = 1.75073 + 0.49597 Log$_e$C] film-coated EQCM electrode, (b) Calibration curve for rebinding of analyte molecule of MIP-coated EQCM electrode at various concentrations of analyte [Freq Shift (Hz) = 53.06425–4.40029 C (nM); R^2 = 0.98867; RSD = 2.01%]. Error bars represent the standard deviation.

Dıaz-Garcıa, 2007; Yusof et al., 2013; Umpleby et al., 2001; Wang et al., 2014; Ansell, 2015). The empirical form of the isotherm was recognized as early as 1926 by Freundlich. It describes amount of adsorbed analyte (B) as a power function of concentration of free analyte in solution (C) as:

$$B = aC^m \quad (2)$$

where '*a*' is a binding affinity parameter and *m* is the heterogeneity index. The binding isotherm for polymer was observed to be well modelled by the Freundlich isotherm (FI). More visually convincing is the numerically identical linear regression analysis of the log B versus log F plot (Fig. 3). On rearrangement to logarithmic form, it arranges to

$$\log B = m \log C + \log a \quad (3)$$

On plotting log B versus log C, *a* and *m* are obtained for a particular system under examination. Fig. 3 demonstrates the binding isotherms for MIP and NIP, where change in resonating frequency (log Δf) noted for MIP and NIP coated EQCM electrode on exposing the respective electrodes with analyte solution with varying concentration (log C). Slope of this isotherm *i.e.* *m* is less than 1 (m = −1.80) indicating that

system is heterogeneously (for homogenous system $m = 1$). Further on comparison of quantitative value of 'a' for MIP and NIP coated electrodes; showing binding affinity of imprinted cavities (6.67 for MIP and 5.75 for NIP) substantiates the imprinting effect, *i.e.* formation of specific binding sites *via* molecular imprinting (Table S3). Consequently, as claimed by molecular imprinting fraternity, formation of artificial analogues of enzymes, antibodies or other biological entities is possible by imprinting technique.

In general, MIPs, where cavities with high binding affinity are distributed in homogeneous manner, are ideally attributable to their highest selectivity for the analyte molecules (Umpleby et al., 2004).

3.9. Analytical applications

The calibration plot for epitope-imprinted EQCM sensor is represented in Fig. 3(b). A linear relationship was obtained in the concentration range from 10 to 140 nM; the linear regression equation is Freq Shift (Hz) = 53.06425–4.40029 C (nM) with a correlation coefficient (R^2) of 0.9886 and relative standard deviation (RSD) of 2.01%. Standard error bar for concentration rebinding of analyte to MIP and NIP modified electrodes are displayed in Fig. 2. Minimum height error bar represents the less uncertain error in the measurement, showing the preciseness of the measurement and supporting the reproducibility of the developed sensor. This calibration curve was used to calculate limit of detection (LOD) and limit of quantification (LOQ) for the sensor. It was calculated as 0.161 nM and 0.536 nM respectively, calculated by standard analytical method (Skoog et al., 1998).

3.10. Cross - selectivity study towards their analogues, proteins and real sample

To evaluate the selectivity of this MIP sensor for epitope (LDIYTTLARDMAAIP (LP-15)), cross reactivity for functionally and structurally comparable interfering agents like other epitope sequences with mismatched amino acids sequence LP-13, KC-14, VC-13, KW-12, GW-10 and proteins present in blood plasma like albumin and globulin were chosen. The response of resonant frequency of modified EQCM electrode is shown in Fig. 4. The closest sequence, *i.e.* LP-13, in which only 2 amino acids are missing from that of analyte sequence LP-15, shows binding respective to only −89.56 Hz (arising from non-specific interactions) in comparison to −389 Hz for LP-15 endorsing the selectivity of imprinted sites only for analyte sequence LP-15. This suggests that the exact 3D contour is required for firm and specific binding in cavities generated by orientation of monomers induced through analyte sequence (LP-15). While other peptide sequences and even plasma proteins are not able to show any binding although sequences are comprised of the same amino acid residues but placed and aligned differently.

The proposed MIP sensor was validated by applying to their real samples of Hansen diseases like multi-bacillary Hansen disease (MBHD), pauci-bacillary Hansen disease (PBHD) and lepromatous leprosy hansen disease (LLHD). Fig. 5 presents bar diagram of respective disease sample with their resonating frequency of EQCM response; results shows PBHD1 has highest binding affinity (−230 Hz) towards MIP sensor while healthy human blood samples gives positive shift in frequency of EQCM response (Fig. 5). This verifies that this MIP-EQCM sensor is not affected by 'matrix effect' of 'real' blood samples. Hence, the objective of this study to develop a sensor for bacteria causing leprosy is achieved. This will be able to detect the bacteria at an early stage when their level in blood is at rock-bottom as LOD obtained is 0.161 nM. Hence the disease could be handled and taken care of at an early stage before it becomes rampant.

3.11. Regeneration, reproducibility and stability of MIP sensor

Reusability of MIP sensor is important for practical sensing applications and construction of detection platforms. The proposed sensor was reused after 30 days with reproducible data (Fig. S13). Multiple use of MIP sensor with repetitive extraction (regeneration of imprinted cavity) and binding cycles were not able to compromise the sensitivity and selectivity of sensing matrix without significant loss of detection levels. The changes in current were almost similar and also optimized at same concentration level on electrode surface which indicate excellent reusability of MIP sensor.

4. Conclusion

In this work, a piezoelectric electrochemical MIP film EQCM sensor

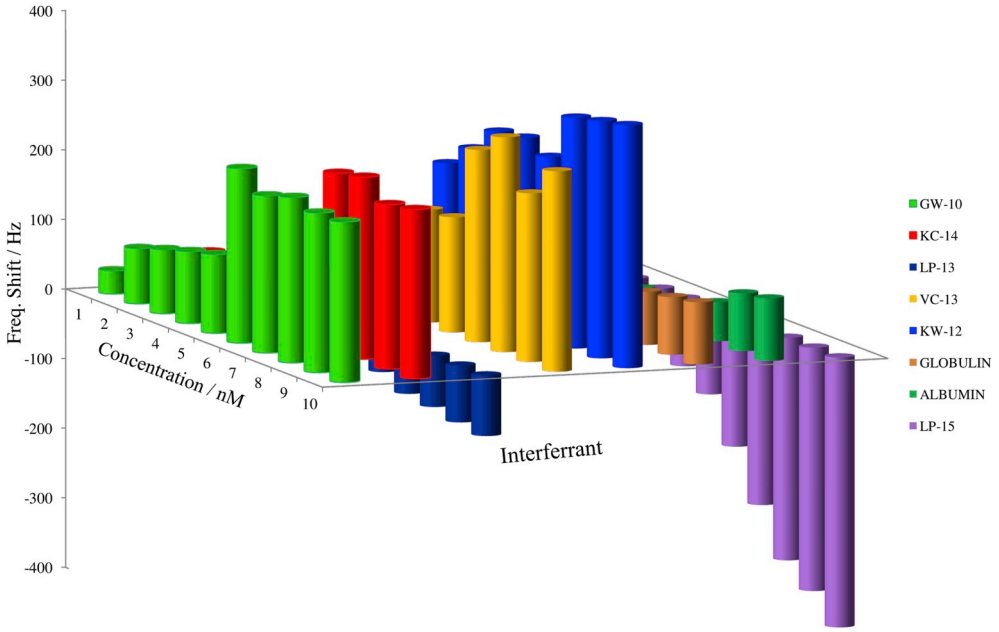

Fig. 4. Response of rebinding on MIP film-coated EQCM electrode for analyte and its structural analogues and some proteins at various concentrations under optimized parameters [1. LP-15; 2. LP-13; 3. GW-10; 4. KC-14; 5. VC-13; 6. KW-12; 7. Globulin; and 8. albumin].

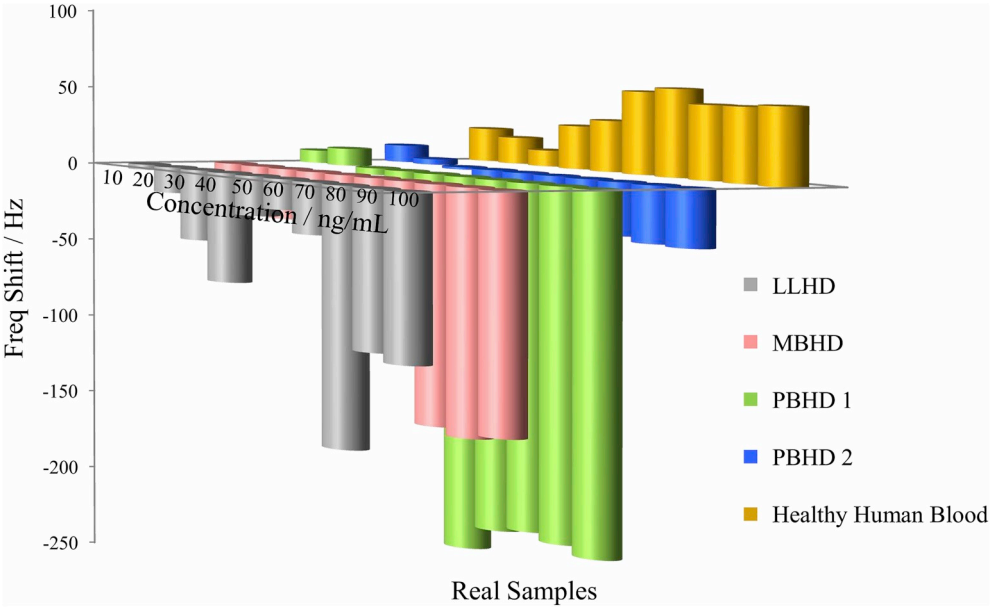

Fig. 5. Rebinding of real blood samples of infected patients and healthy human beings over prepared MIP EQCM sensor (LLHD, MBHD, PBHD1, PBHD2 and healthy human blood].

used to detect epitope of *Mycobacterium leprae* bacteria was fabricated and first developed co-polymerization of *p*-ATP, 3-sulphopropyl methacrylate potassium salt and benzyl methacrylate with the electropolymerization in the presence of analyte (LP-15) molecules which exhibits an excellent detection, with a high sensitivity, enhanced affinity, stability, and rapid recognition towards analyte. MIP was successfully developed on gold surface of EQCM electrode by using multiple functional monomers used as polymeric format for imprinting. The obtained MIP represented high affinity towards analyte (LP-15) recognition. The resultant MIPs EQCM sensor had a fairly thin imprinting layer, which enables fast adsorption kinetics. Binding isotherms followed Freundlich isotherm model representing heterogeneity of adsorption cavities. Binding isotherm parameters as well as imprinting factor confirms the suitability of imprinted matrix over non-imprinted matrix. Moreover, various epitope sequences and proteins were also examined for MIPs-coated film showing selective adsorption toward epitope sequence LDIYTTLARDMAAIP. The excellent detection limits, 0.161 nM are promising for determination of trace amount of analyte facilitating detection of bacteria at an early stage when their level in blood is at primal stage, before it reaches to a substantial infectious level. The developed method exhibited good analytical performance in terms of high sensitivity, selectivity and high percent of recovery. Furthermore, the chemosensor has not only showed good selectivity, but also showed selective recognition toward real blood samples of *Mycobacterium leprae* bacteria infected blood, both suggesting its potential in practical applications. This method provides an alternative method to detect *Mycobacterium leprae* through blood sample and can be used as a diagnostic tool sensor in future.

CRediT authorship contribution statement

Archana Kushwaha: Conceptualization, Data curation, Formal analysis, Investigation, Methodology, Writing - original draft. **Juhi Srivastava:** Data curation, Formal analysis. **Ambareesh Kumar Singh:** Methodology, Supervision, Project administration. **Richa Anand:** Software, Data curation. **Richa Raghuwanshi:** Conceptualization, Funding acquisition, Supervision, Writing - review & editing. **Tulika Rai:** Resources. **Meenakshi Singh:** Conceptualization, Funding acquisition, Investigation, Project administration, Resources, Supervision, Writing - review & editing.

Declaration of competing interest

The authors declare that they have no known competing financial interests or personal relationships that could have appeared to influence the work reported in this paper.

Acknowledgements

The work was supported by DST-SERB, New Delhi [Grant no. EMR/2016/005245].

Appendix A. Supplementary data

Supplementary data to this article can be found online at https://doi.org/10.1016/j.bios.2019.111698.

References

Lopez-Puertollano, Cowen T., Garcia-Cruz, Piletska E., Abad-Somovilla, A., Abad-Fuentes, Piletsky S., 2019. ChemNanoMat 5, 651–657.
Ansari, S., Masoum, S., 2019. Trends Anal. Chem. 114, 29–47.
Ansell, R.J., 2015. Characterization of the binding properties of molecularly imprinted polymers. In: In: Mattiasson, B., Ye, L. (Eds.), Molecularly Imprinted Polymers in Biotechnology, Advances in Biochemical Engineering/Biotechnology, vol. 150. Springer International Publishing, pp. 51–93.
Crespilho, F.N., Zucolotto, V., Brett, C.M., Oliveira, O.N., Nart, F.C., 2006. J. Phys. Chem. B 110, 17478–17483.
Du, J., Wang, Y., Zhou, X., Xue, Z., Liu, X., Sun, K., Lu, X., 2010. J. Phys. Chem. C 114, 14786–14793.
Eichelmann, K., González, S.G., Salas-Alanis, J.C., 2013. Ocampo-candiani. J. Actas Dermo-Sifiliográficas 104, 554–563.
Garcıa-Calzon, J.A., Dıaz-Garcıa, M.E., 2007. Sens. Actuators B 123, 1180–1194.
Gupta, N., Shah, K., Singh, M., 2016. J. Mol. Recognit. 29, 572–579.
Gupta, N., Singh, R.S., Shah, K., Prasad, R., Singh, M., 2018. J. Mol. Recognit. 31, 2709–2717.
Han, X.Y., Sizer, K.C., Thompson, E.J., Kabanja, J., Li, J., Hu, P., Gómez-Valero, L., Silva, F.J., 2009. J. Bacteriol. 191, 6067–6074.
Held, P., 2003. Quantitation of Peptides and Amino Acids with a Synergy™ HT Using UV Fluorescence. B.-T. Instruments, Winooski, VT.
Iskierko, Z., Sharma, P.S., Noworyta, K.R., Borowicz, P., Cieplak, M., Kutner, W., Bossi, A.M., 2019. Anal. Chem. 91, 4537–4543.
Kumar, S.S., Joseph, J., Phani, K.L., 2007. Chem. Mater. 19, 4722–4730.
Lukkari, J., Kleemola, K., Meretoja, M., Ollonqvist, T., Kankare, J., 1998. Langmuir 14, 1705–1715.
Martins, M.V.S.B., Guimaraes, M.M.D.S., Spencer, J.S., Hacker, M.A.V.B., Costa, L.S., Carvalho, F.M., Geluk, A., Schip, J.J.V.P., Pontes, M.A.A., Goncalves, H.S., Morais, J.P.D., Bandeira, T.J.P.G., Pessolani, M.C.V., Brennan, P.J., Pereira, G.M.B., 2012.

PLoS Neglected Trop. Dis. 6, e1616–1627.
Nishino, H., Huang, C.S., Shea, K.J., 2006. Angew. Chem. Int. Ed. 118, 2452–2456.
Raj, C.R., Kitamura, F., Ohsaka, T., 2001. Langmuir 17, 7378–7386.
Skoog, D.A., Holler, F.T., Neiman, T.A., 1998. Principles of Instrumental Analysis, fifth ed. Harcourt brace college publisher, Florida, pp. 13–14.
Spencer, J.S., Dockrell, H.M., Kim, H.J., Marques, M.A., Williams, D.L., Martins, M.V., Martins, M.L., Lima, M.C., Sarno, E.N., Pereira, G.M., Matos, H., 2005. J. Immunol. 175, 7930–7938.
Spivak, D., 2005. Polymers. Adv. Drug Deliv. Rev. 57, 1779–1794.
Tchinda, R., Tutsch, A., Schmid, B., Sussmuth, R.D., Altintas, Z., 2019. Biosens. Bioelectron. 123, 260–268.
The Hindu Delhi Ed. 10 Feb 2019, 1.
Umpleby, R.J., Baxter, S.C., Chen, Y., Shah, R.N., Shimizu, K.D., 2001. Anal. Chem. 73, 4584–4591.
Umpleby, R., Baxter, S., Rampey, A., Rushton, G., Chen, Y., Shimizu, K., 2004. J. Chromatogr. B 804, 141–149.
Vittal, R., Gomathi, H., 2002. J. Phys. Chem. B 106, 10135–10143.
Wang, J., Dai, J., Meng, M., Song, Z., Pan, J., Yongsheng, Y., Li, C., 2014. J. Appl. Polym. Sci. 40310, 1–10.
WHO, 2004. Leprosy Elimination Project: Status Report 2002–2003. WHO, Geneva.
Yang, Y.Q., He, X.W., Wang, Y.Z., Li, W.Y., Zhang, Y.K., 2014. Biosens. Bioelectron. 54, 266–272.
Yusof, N.A., Rahman, SK Ab, Hussein, M.Z., Ibrahim, N.A., 2013. Polymer 5, 1215–1228.